Progress In Electromagnetics Research C, Vol. 132, 11–21, 2023

Simplified Design Procedure for Fourth-Order Coupled-Resonator Bandpass Filter

Mai A. Salah[1, 2], Eman M. Eldesouki[1], Ahmed M. Attiya[1], and Walid S. El-Deeb[2, *]

Abstract—This paper presents a new simplified procedure to design a fourth-order coupled resonator filter. This procedure does not require the calculation of complicated eigenvalues to develop the required coupling matrix. It starts with studying the effects of different coupling mechanisms on the performance of the overall filter structure. Then, these coupling mechanisms are combined to obtain the design of the required filter. This procedure may be more suitable for machine learning procedure to design coupled-resonator filters. The proposed method is used to design a substrate integrated waveguide (SIW) bandpass filter for sub-six GHz 5G applications. The designed SIW bandpass filter operates in the frequency range from 3.7 GHz to 3.98 GHz which covers the new C-band 5G network with a fractional bandwidth (FBW) of 28% and is centered at 3.84 GHz. This filter is fabricated and measured for verification.

1. INTRODUCTION

Bandpass filters mainly consist of resonators coupled to each other by inductive or capacitive coupling elements. Coupled resonator filters have found wide applications in modern wireless communication systems [1, 2], radar systems [3, 4], and laboratory measurement equipment [5]. There is a general technique for designing these filters that can be applied to any type of resonator regardless of its physical structure [6]. This technique is based on determining the coupling matrix for the coupled resonators arranged in a specific topology. The methods for deriving the coupling matrices are extensively discussed in [7–11]. These methods are based on direct synthesis combined with matrix rotations [7–9] or based on optimization of the coupling matrix [10, 11].

Using the coupling matrix method [12, 13] to tune a coupled resonator filter is a complicated problem. Conventional steps to design a bandpass filter starts with calculating the coupling matrix. The coupling element between the input/output port and the first/last resonator depends on the external quality factor of these resonators when they are connected to input/output loads. Moreover, the remaining coupling elements of the coupling matrix are related to the coupling coefficients between different cavities. To obtain the external quality factors and coupling coefficients, different simulations are performed to present the relation between these parameters and the physical dimensions of the coupling parts between resonators, for example, the width of the slot between cavities. Then, according to the required values of the coupling matrix elements, the required dimensions of the coupling parts for a specific response are determined from these simulated results. The disadvantage of this technique is that the obtained dimensions by simulation are obtained for the case of isolated resonators. When all these resonators are coupled together to develop the required structure of the bandpass filter, the coupling mechanism is slightly changed. Thus, after developing the complete structure, it would be required to perform fine tuning to obtain the required performance.

Received 6 February 2023, Accepted 24 March 2023, Scheduled 7 April 2023

* Corresponding author: Walid Saber El-Deeb (wseldeeb@ucalgary.ca).

[1] Microwave Engineering Department, Electronics Research Institute (ERI), Cairo, Egypt. [2] Electronics and Communications Engineering Department, Faculty of Engineering, Zagazig University, Egypt.

This paper presents simple steps to realize a fourth-order coupled resonator bandpass filter. In this case, the physical dimensions of the complete filter are extracted directly from different coupling mechanisms between four coupled waveguide cavities and the required bandpass performance. This method does not depend on calculating the coupling matrix. This procedure may be more suitable for deep learning and direct optimization techniques to design coupled-resonator filters [14–16].

The proposed procedure starts with studying a single cavity resonator and its equivalent RLC circuit model. Then, two coupled cavity resonators are also investigated to adjust the start and stop frequencies of the bandpass range. After that, the effects of different coupling mechanisms among the four coupled resonators on the performance of the overall filter structure are investigated separately. Then, these coupling mechanisms are combined to obtain the final design of the required filter. Numerical simulations of the resonators and bandpass filter are developed by using High Frequency Structure Simulator (HFSS) and advanced design system (ADS). This procedure is initially studied on rectangular cavities with solid conducting walls where there is no leakage from the sides, and it is possible to adjust the coupling apertures for the required values. However, for experimental verification, these solid conducting walls are replaced by arrays of via holes for SIW cavities. Although the SIW configuration introduces slight degradation compared to cavities with solid conducting walls, it is used here to simplify the manufacturing process.

The proposed filter in this paper is a bandpass filter in the frequency range from 3.7 to 3.98 GHz which covers the new C-band 5G network with an attenuation of more than 20 dB in the frequency range from 4.2 to 4.4 GHz. This attenuation represents the main concern in the present design for the proposed application. These specifications are mainly required to reduce the interference of the C-band 5G network and radio altimeter systems in aircrafts [18].

This paper is organized as follows: Section 2 presents the different coupling mechanisms between cavity resonators. Section 3 presents the design procedures of the fourth-order coupled resonators filter. Section 4 presents the fabricated design and the experimental results of the bandpass filter. Finally, the conclusion of this work is included in Section 5.

2. DESIGN AND ANALYSIS OF A FOURTH ORDER COUPLED-RESONATOR FILTER

In this section, the single cavity resonator and its equivalent RLC circuit model are studied. In addition, two coupled cavity resonators are also studied to adjust the start and stop frequencies of the operating band. Four resonators are coupled in a specific topology to construct the required filter geometry. Then, the effects of different coupling mechanisms among these four coupled resonators are investigated on the performance of the overall filter structure.

2.1. Single Cavity Resonator

Figure 1(a) shows a rectangular cavity resonator, R_1, which can be implemented as a section of a rectangular waveguide resonator filled with a dielectric constant, ε_r, with dimensions a, b and height h,

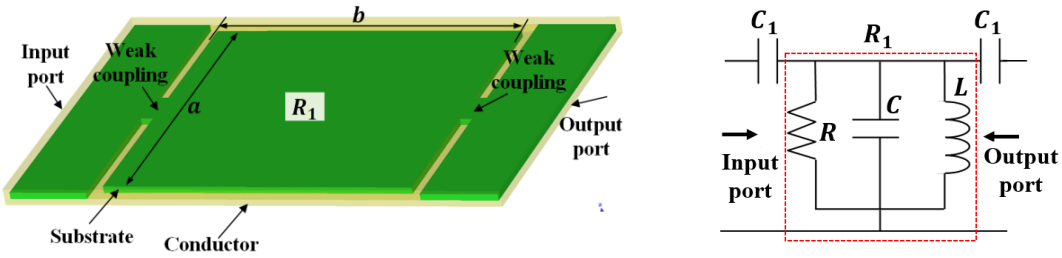

Figure 1. Single cavity resonator; (a) Waveguide model and (b) equivalent parallel RLC circuit model.

where $h < b \leq a$. The resonance frequency of the dominant, TE_{101}, mode of this rectangular cavity is:

$$F_{101} = \frac{c}{2\pi\sqrt{\varepsilon_r}}\sqrt{\left(\frac{\pi}{a}\right)^2 + \left(\frac{\pi}{b}\right)^2} \tag{1}$$

where c is the speed of light in free space. The unloaded quality factor of this cavity resonator is dominated by the dielectric loss since the conductor loss is much less in the proposed frequency range in the sub-six GHz band of 5G. Thus, the unloaded quality factor can be approximated as:

$$Q_0 \cong \frac{1}{\tan\delta} \tag{2}$$

where $\tan\delta$ is the loss tangent of the filling dielectric material.

This cavity resonator is connected by weak coupling to the input and output ports to determine its resonance response. For the present case, the proposed resonance frequency is 3.83 GHz. The filling dielectric material is assumed to be Rogers RT/Droid 5880 of $\varepsilon_r = 2.2$ and $\tan\delta = 0.0009$. The dimensions of the rectangular cavity which correspond to the resonance frequency of 3.83 GHz would be $a = b = 37.34$ mm, and the height is assumed to be $h = 0.787$ mm. This cavity resonator is coupled to two waveguide ports through narrow coupling slots as shown in Fig. 1(a). The width of the coupling slot in the present case is 5 mm.

On the other hand, Fig. 1(b) shows the equivalent parallel RLC circuit resonator. This parallel RLC circuit is connected to the input and output ports via small coupling capacitors, c_1, which corresponds to the required week coupling. The value of c_1 in the present case is 0.01 pF. The resonance frequency of a parallel RLC is given by:

$$f_o = \frac{1}{2\pi\sqrt{LC}} \tag{3}$$

and the unloaded quality factor of a parallel RLC circuit is:

$$Q_o = 2\pi f_o RC = \frac{R}{2\pi f_0 L} \tag{4}$$

To calculate the parameters of the equivalent parallel RLC circuit, the value of the capacitance C is assumed to be 10 pF. Then, the value of the inductance L is determined from the resonance frequency. After that, the value of the resistance R is determined from the unloaded quality factor. Thus, the inductance L is 172.32 pF, and the resistance R is 4150 Ω.

Figure 2 shows the transmission response of the simulated rectangular cavity resonator and its equivalent RLC circuit resonator model. In this figure, the transmission coefficient is characterized by a single peak value at the resonance frequency. The coupling capacitors in the equivalent circuit are adjusted to obtain nearly the same peak of the transmission response of the rectangular cavity.

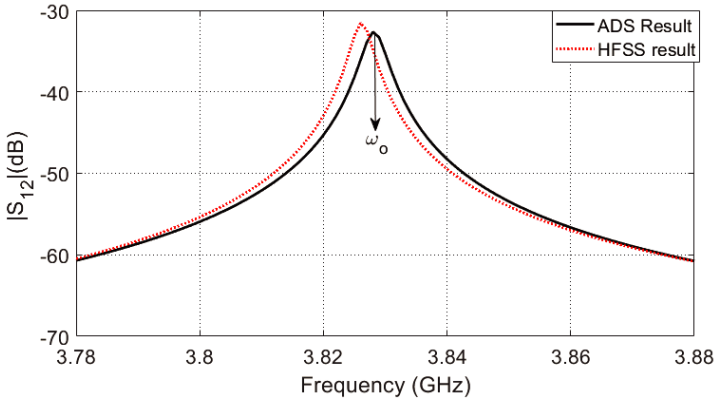

Figure 2. The frequency response of the single waveguide cavity and its equivalent RLC circuit resonator.

2.2. Performance of Two Coupled Cavities

The performance of two coupled cavities was previously discussed in detail in [17]. Fig. 3(a) shows the two coupled waveguide cavity resonators, R_1 and R_2, through a coupling aperture, W_{12}, and weak coupling at the input and output ports. The equivalent RLC circuit model of these coupled resonators is shown in Fig. 3(b). It consists of two parallel RLC resonators coupled via a coupling capacitor, C_{12}. Weak coupling capacitors C_1 are used at the input and output ports. The coupling coefficient is mainly controlled by adjusting the coupling aperture between the waveguide resonators, W_{ij}, which corresponds to adjusting C_{ij}, in the equivalent RLC circuit.

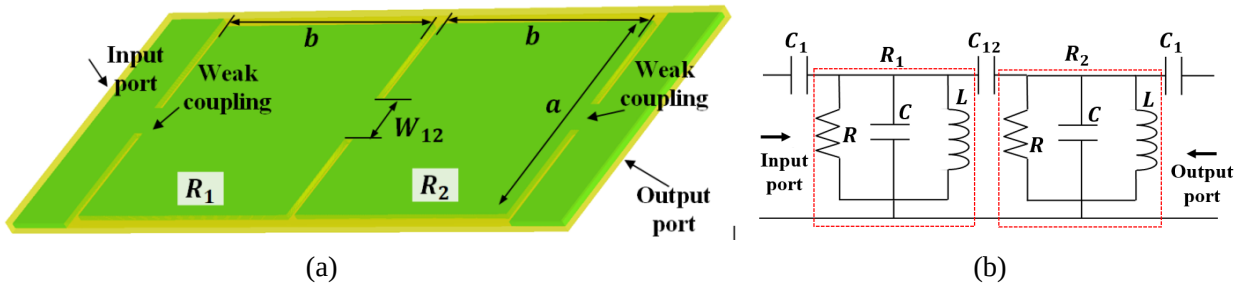

Figure 3. Two capacitive coupled resonators; (a) Waveguide model and (b) equivalent RLC circuit model.

It can be noted that the coupling between the two resonators introduces two peaks in the transmission coefficient as shown in Fig. 4. For the present configuration, the peak at the higher frequency would be nearly at the original resonance frequency of the single resonator while the other peak would be below this resonance frequency. The difference between these two peaks increases by increasing the coupling between the two coupled resonators. This property is verified analytically in a closed form for the equivalent RLC resonators [17]. In the present case, the value of the coupling aperture, W_{12}, is 10 mm, and the weak coupling apertures at the input and output ports are 5 mm. For the equivalent RLC circuit, the value of the coupling capacitor, C_{12}, is 0.1 pF, and the weak coupling capacitors at the input and output ports are 0.01 pF.

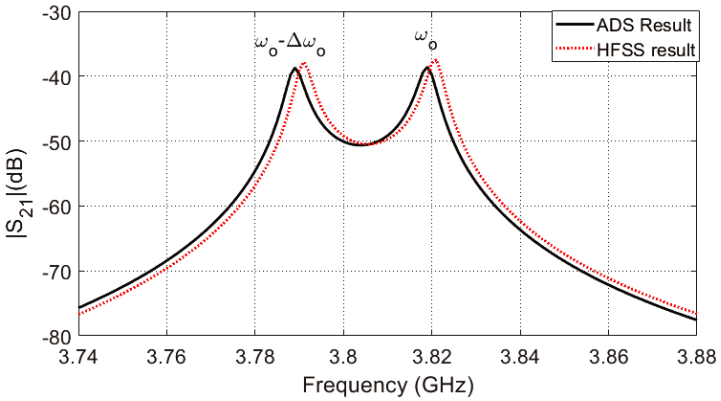

Figure 4. The response of the simulated two coupled resonators and the RLC circuit resonators.

3. FOURTH ORDER COUPLED CAVITY RESONATOR CONFIGURATION

The configuration of the four waveguide cavity resonators bandpass filter is shown in Fig. 5(a). It consists of four coupled resonators, R_1, R_2, R_3, and R_4. Each cavity resonator has dimensions of $a \times b$ corresponding to resonance frequency as given in (1). Due to the symmetry of the proposed

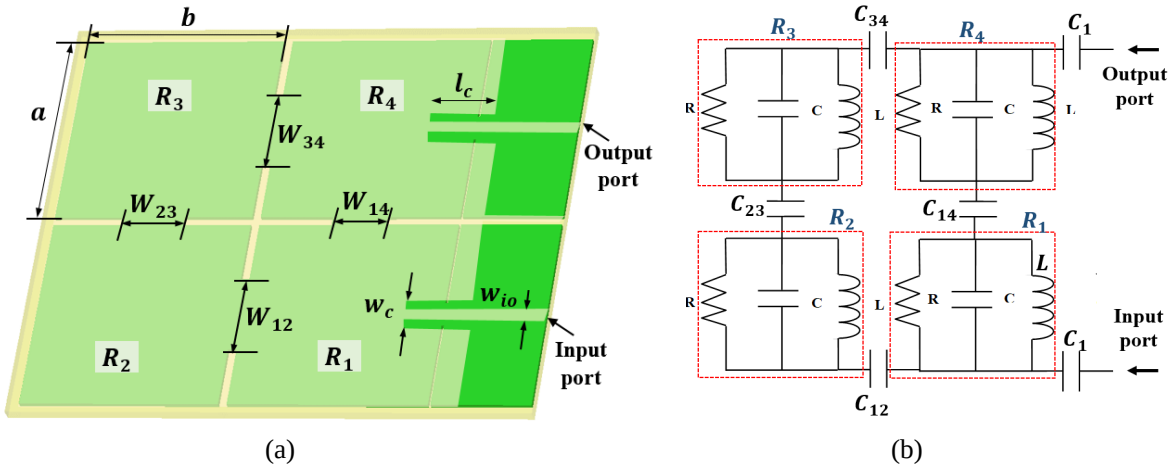

(a) (b)

Figure 5. (a) Geometry of the proposed 4th order waveguide resonator bandpass filter. (b) Equivalent RLC circuit of the proposed filter.

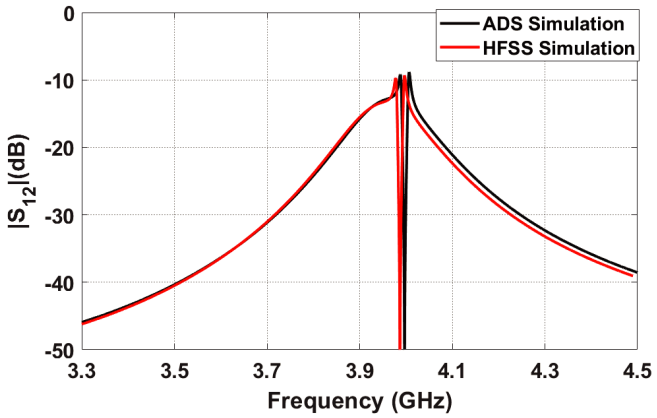

Figure 6. The response of 4th order waveguide coupled resonators and their equivalent RLC circuit model with all weak coupling aperture.

configuration, the coupling apertures, W_{12} and W_{34}, are equal. Two microstrip lines of length, L_C, and width, w_{io}, are used for feeding the input and output cavities. The length of these microstrip lines is adjusted to control the external quality factor of these cavities, and their width is chosen to satisfy the characteristic impedance of 50 Ω. External quality factor plays a critical role in impedance matching at the passband. The equivalent RLC circuit of the fourth-order coupled resonators is shown in Fig. 5(b). It consists of four parallel RLC resonators coupled via coupling capacitors, C_{12}, C_{23}, C_{34}, and C_{14} with coupling capacitors, C_1, at the input and output ports.

The effects of different coupling mechanisms for this configuration are studied separately. The first step in this study is the case where all the coupling apertures have the same width, $w_{ij} = 6.5$ mm, which corresponds to weak coupling between all resonators and the length of the microstrip line inside the input and output cavities, $L_c = 13$ mm. In this case, the obtained transmission coefficient is characterized by two peaks separated by a deep null centered nearly at the resonance frequency of the cavity resonator as shown in Fig. 6. A similar performance is obtained by using the equivalent circuit with weak coupling capacitors, $C_{ij} = 0.1$ pF, as shown in Fig. 6.

In the following step, the coupling between the resonators, R_2 and R_3, is increased while the remaining couplings are maintained to be a small value. Fig. 7 shows the effect of increasing w_{23}. It can be noted that the separation between the two peaks of the transmission coefficient increases by increasing the coupling between the resonators R_2 and R_3. The upper-frequency peak is still close to

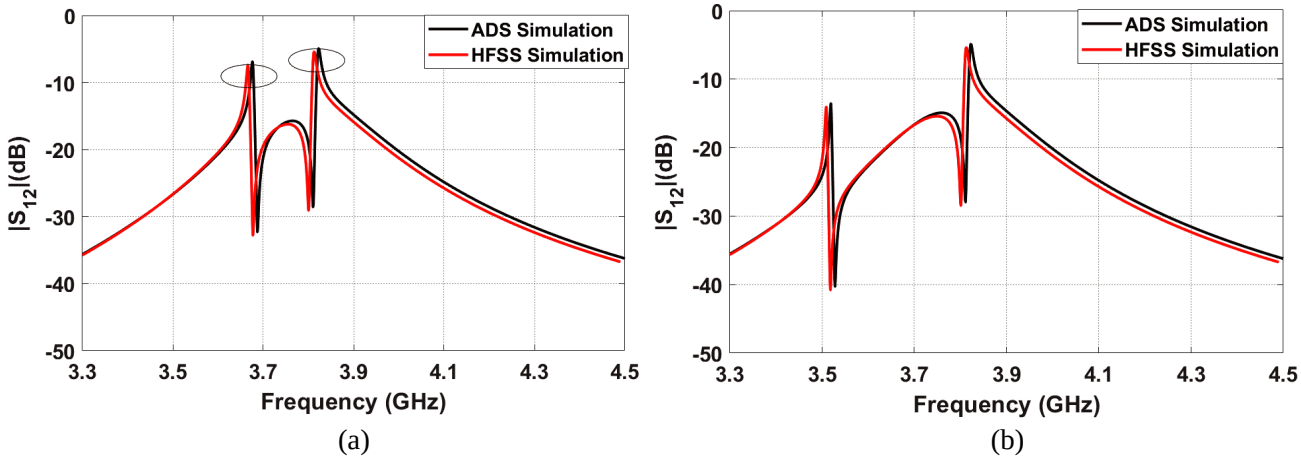

Figure 7. The effect of changing the coupling between R_2, R_3 on the response of 4^{th}-order waveguide coupled-resonators and their equivalent RLC circuit. (a) $w_{23} = 9\,\text{mm}$, $C_{23} = 0.4\,\text{pF}$ and (b) $w_{23} = 11.5\,\text{mm}$, $C_{23} = 0.9\,\text{pF}$.

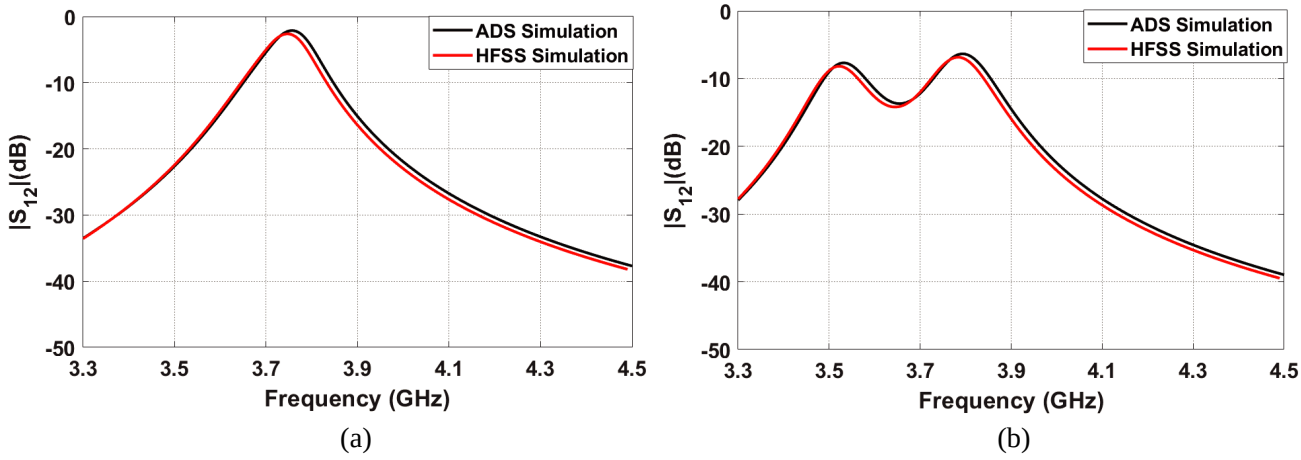

Figure 8. The effect of changing the coupling between R_1, R_2 on the response of 4^{th}-order waveguide coupled-resonators and their equivalent RLC circuit. (a) $w_{12} = 10\,\text{mm}$, $C_{12} = 0.4\,\text{pF}$ and (b) $w_{12} = 14\,\text{mm}$, $C_{12} = 0.9\,\text{pF}$.

the resonance frequency of the original cavity. It can also be noted that the lower frequency peak of the transmission coefficient becomes smaller than the upper-frequency peak as the coupling between the resonators R_2 and R_3 is increased to a large value. It is found that the maximum bandwidth of the bandpass filter which can be obtained by using this configuration is limited to the maximum coupling between R_2 and R_3 which does not introduce a significant difference between the magnitudes of the two peaks of the transmission coefficient. This performance is also obtained by using the equivalent RLC circuit by changing the value of the coupling capacitor C_{23}.

Then the effect of increasing w_{12} is studied while w_{23} and w_{14} are maintained to be 6.5 mm. Fig. 8 shows the performance of the transmission coefficient in this case. It can be noted that by increasing w_{12}, the null of the transmission coefficient of the case of all week coupling is replaced by a peak on the transmission coefficient as shown in Fig. 7(a). For larger w_{12}, this peak in transmission coefficient is separated into two peaks as shown in Fig. 7(b). The upper-frequency peak is also near the resonance frequency of the original cavity resonator. The magnitude of the lower frequency peak of the transmission coefficient is also slightly less than the corresponding one of the upper-frequency peak.

The effect of increasing both w_{12} and w_{23} on the transmission coefficient is shown in Fig. 9. It

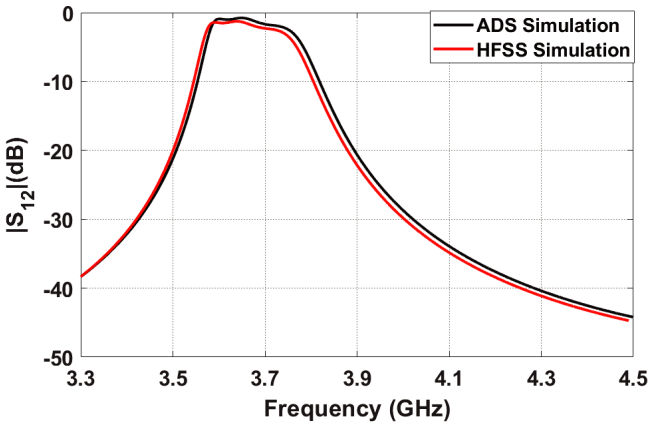

Figure 9. Frequency response of 4$^{\text{th}}$-order waveguide coupled-resonators and their equivalent RLC circuit resonators with $w_{12} = 14\,\text{mm}$, $w_{23} = 11.5\,\text{mm}$ and $C_{12} = 0.4\,\text{pF}$, $C_{23} = 0.4\,\text{pF}$.

is noted that the performance of a bandpass filter could be slightly obtained in this case. However, the insertion loss is still slightly large. This insertion loss could be improved by tuning the coupling between R_1 and R_4 and also by adjusting the external quality factor of R_1 and R_4 as discussed in the following parts. It is also noted that the center frequency of the passband is less than the resonance frequency of the single resonator. Thus, the upper frequency of the passband is close to the resonance frequency of the resonator. Hence, the resonance frequency of the single resonator should be adjusted to be $f_0' = f_0 + \frac{\Delta f}{2}$ where f_0 and Δf are the center frequency and the bandwidth of the required passband, respectively.

The next step after obtaining the starting performance of the bandpass filter is to adjust the coupling between the input and output resonators R_1 and R_4 by increasing the width of the coupling aperture, w_{14}. Fig. 10 shows the effect of increasing w_{14} to 9.75 mm. It can be noted that the transmission response in the passband, in this case, is nearly constant compared to the previous case in Fig. 9. It is also noted that increasing the coupling between R_1 and R_4 improves the matching at the lower frequency band. Moreover, it can be noted that the center frequency of the passband is shifted below the resonance frequency of the single cavity such that the upper $-3\,\text{dB}$ frequency limit is less

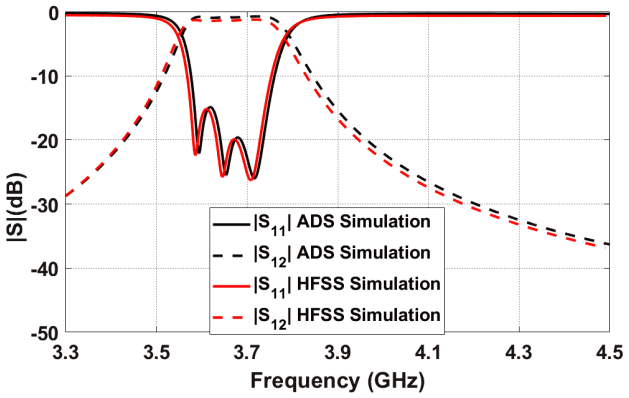

Figure 10. Frequency response of 4$^{\text{th}}$-order waveguide coupled-resonators and their equivalent RLC circuit resonator with effecting of changing the coupling between the R_1 and R_4: $w_{12} = 14\,\text{mm}$, $w_{23} = 11.5\,\text{mm}$, $w_{14} = 9.75\,\text{mm}$, and $L_c = 13\,\text{mm}$.

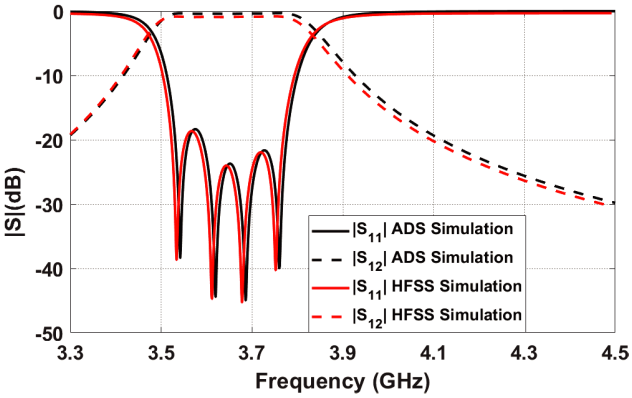

Figure 11. Frequency response of 4$^{\text{th}}$-order waveguide coupled-resonators and their equivalent RLC circuit resonator with effecting of changing the input and output coupling $w_{12} = 14\,\text{mm}$, $w_{23} = 11.5\,\text{mm}$, $w_{14} = 9.75\,\text{mm}$, and $L_c = 12\,\text{mm}$.

than this resonance frequency.

The final step in the design is adjusting the external quality factors of the input and output resonators to the feeding transmission lines. In the present configuration, this can be obtained by adjusting the length, L_c, of the feeding microstrip line inside the cavity as shown in Fig. 5. Fig. 11 shows the effect of decreasing L_c to be 12 mm. It can be noted that adjusting the external quality factor of the input and output resonators by adjusting the length L_c improves the matching passband in the upper-frequency limit as shown in Fig. 11. It can also be noted that the upper frequency of the passband is increased by adjusting the external quality factor.

Based on the above results it can be concluded that the design steps of a four-coupled resonator bandpass filter are as follows:

1- The center frequency of the single cavity is chosen to be above the upper limit of the passband by nearly half the required bandwidth because the coupling between the cavities shifts the passband to a lower frequency than the resonance of the single cavity.

2- The coupling between R_2 and R_3 controls the bandwidth of the passband by two peaks in the transmission coefficients. As this coupling increases, the passband increases. This coupling introduces two peaks in the transmission coefficient. This coupling is increased to the point where these two peaks would be at the limits of the passband.

3- The coupling between R_1 and R_2 (which equals the coupling between R_3 and R_4) introduces the passband. It should be increased to reach the two peaks obtained by increasing the coupling between R_2 and R_3.

4- The combination of increasing the coupling of R_2 and R_3 and the coupling between R_1 and R_2 (which equals the coupling between R_3 and R_4) introduces the main performance of the bandpass filter. The center frequency in this case is shifted below the resonance frequency of the single cavity. Thus, the resonance cavity should be designed at a higher frequency than the required center frequency of the proposed bandpass filter.

5- The coupling between R_1 and R_4 improves the performance of the passband and the matching at the lower frequency limit.

6- Adjusting the external quality factors of R_1 and R_4 by adjusting the feeding ports improves the performance of the passband in the upper-frequency limit and increases the passband.

4. EXPERIMENTAL RESULTS

The above-mentioned steps are used to design a bandpass filter based on four coupled cavity resonators. The cavity resonators are realized by using the SIW technique. It should be noted that the previous analysis in the above section is based on rectangular cavities with solid conducting walls. SIW is more suitable for experimental implementation. However, SIW has two main disadvantages: slight leakage and difficulty to adjust the coupling apertures to their exact values. These effects could introduce a slight degradation on the overall performance of the designed filter. The dimensions of the different parts of the proposed fourth-order SIW-bandpass filter (BPF) shown in Fig. 12 are listed in Table 1. The substrate is Rogers RT/Droid 5880 with a dielectric constant, $\epsilon_r = 2.2$, loss tangent of 0.009, and substrate thickness of $h = 0.787$ mm. The bandwidth of the proposed filter lies in the frequency range from 3.7 to 3.98 GHz. Thus, the center frequency is 3.84 GHz. For a single cavity with a resonance frequency at the upper-frequency limit, the length and width of a square SIW resonator would be $a = b = 35.5$ mm. The diameter of the via hole would be $D = 1.5$ mm, and the spacing between the via holes would be $p = 1$ mm. The remaining parameters of the coupled resonator filter are obtained as discussed in the above section.

The designed bandpass filter configuration is simulated by using the HFSS tool. The filter is fabricated and measured for verification. Fig. 13 shows a comparison between measured and fabricated bandpass filters. The difference between the simulated results of Fig. 13 and Fig. 11 is due to replacing the solid conducting walls in Fig. 11 by arrays of via holes in Fig. 13. On the other hand, the slight difference between the measurement and simulation results in Fig. 13 can be explained due to the manufacturing tolerance in the metallic plating of the via-holes for the fabricated filter in addition to the effect of the soldered connectors. However, after all these effects, it can be noted that the simulated

Table 1. Physical dimensions of fourth-order rectangle SIW-bandpass filter.

Symbol	Dimension (mm)	Symbol	Dimension (mm)
w_{io}	1.35	L_c	11
w_c	2.05	a	35.5
w_{12}	13.75	b	35.5
w_{23}	11	D	1.5
w_{14}	10	P	1

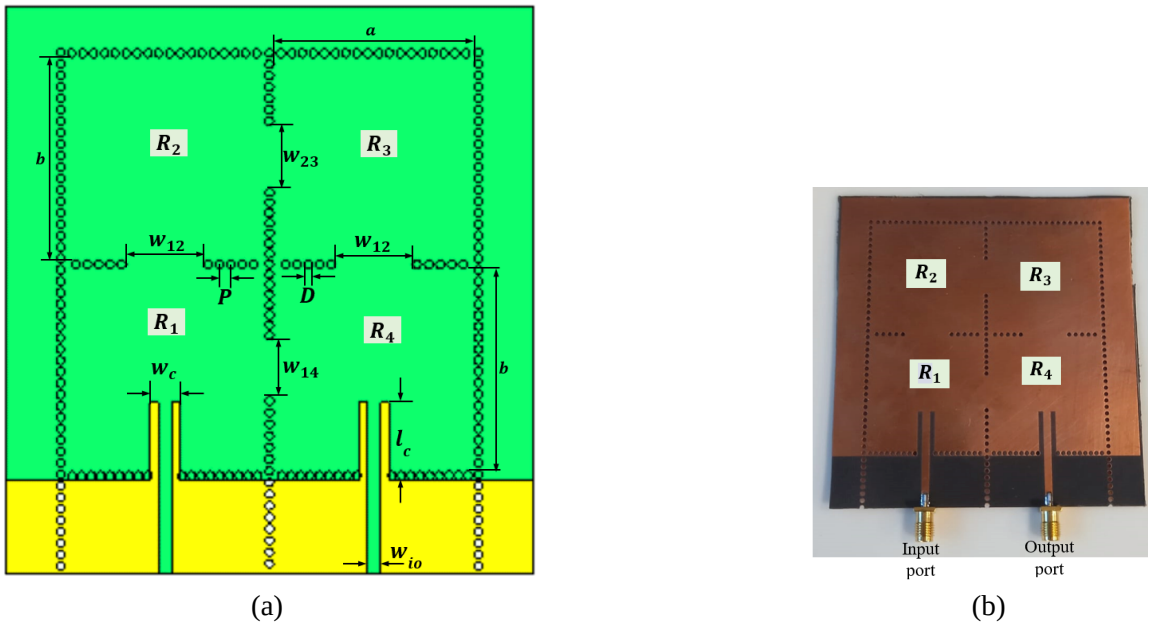

(a) (b)

Figure 12. (a) Geometrical model of the fourth-order SIW bandpass filter. (b) Fabricated SIW bandpass filter.

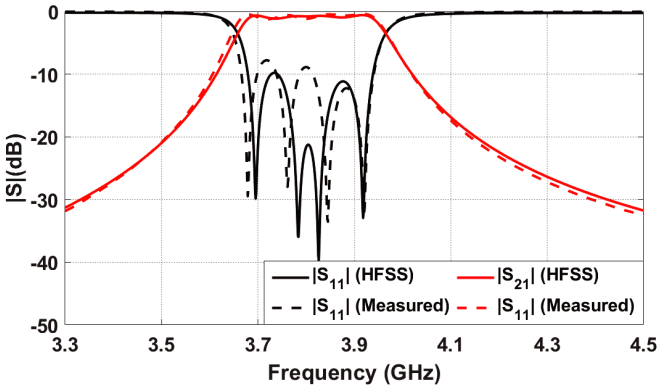

Figure 13. Simulated and measured results of the designed fourth-order bandpass filter.

S_{11} is less than -10 dB in the entire frequency band while the variation of S_{21} is smaller than 0.5 dB. On the other hand, in the band from 2.2 to 4.4 GHz the transmission coefficient is less than -20 dB. These specifications are quite suitable for reducing the interference of the new C-band 5G network from radio altimeter systems.

5. CONCLUSION

This paper presents a new simplified procedure to design a fourth-order coupled resonator filter. It starts with studying the effects of different coupling mechanisms on the performance of the overall filter structure. Then, these coupling mechanisms are combined to obtain the design of the required filter. This simplified method is used to design a fourth-order bandpass filter frequency range from 3.7 to 3.98 GHz. The designed filter is fabricated and measured for verification. The proposed filter is quite suitable for reducing the interference between the C band 5G network and radio altimeter system.

REFERENCES

1. Xu, J., K. Bi, X. Zhai, Y. Hao, and K. D. Mcdonald-Maier, "A dual-band microwave filter design for modern wireless communication systems," *IEEE Access*, Vol. 7, 98786–98791, 2019.
2. Yang, Y. and T. Liu, "Research on microwave filter of wireless communication system based on slot structure," *Nonlinear Optics, Quantum Optics: Concepts in Modern Optics*, Vol. 55, 259–267, 2022.
3. Ismail, N., T. S. Gunawan, T. Praludi, and E. A. Hamidi, "Design of microstrip hairpin bandpass filter for 2.9 GHz–3.1 GHz S-band radar with defected ground structure," *Malaysian Journal of Fundamental and Applied Sciences*, Vol. 14, No. 4, 448–455, 2018.
4. Adli, B., R. Mardiati, and Y. Y. Maulana, "Design of microstrip hairpin bandpass filter for X-band radar navigation," *International Conference on Wireless and Telematics (ICWT)*, 1–6, 2018.
5. Hunter, I. C., L. Billonet, B. Jarry, and P. Guillon, "Microwave filters — Applications and technology," *IEEE Trans. Microw. Theory Tech.*, Vol. 50, No. 3, 794–805, 2002.
6. Hong, J. S. G. and M. J. Lancaster, *Microstrip Filters for RF/Microwave Applications*, John Wiley & Sons, 2004.
7. Lee, J. and K. Sarabandi, "A synthesis method for dual-passband microwave filters," *IEEE Trans. Microw. Theory Tech.*, Vol. 55, No. 6, 1163–1170, 2007.
8. Tamiazzo, S. and G. Macchiarella, "An analytical technique for the synthesis of cascaded N-tuplets cross-coupled resonator microwave filters using matrix rotations," *IEEE Trans. Microw. Theory Tech.*, Vol. 53, No. 5, 1693–1698, 2005.
9. Macchiarella, G. and S. Tamiazzo, "A design technique for symmetric dual band filters," *IEEE MTTS Int. Microw. Symp.*, 115–118, 2005.
10. Atia, W. A., K. A. Zaki, and A. E. Atia, "Synthesis of general topology multiple coupled resonator filters by optimisation," *IEEE MTTS Int. Microw. Symp.*, 821–824, 1998.
11. Nicholson, G. L. and M. J. Lancaster, "Coupling matrix synthesis of cross coupled microwave filters using a hybrid optimisation algorithm," *IET Microw. Antennas Propag.*, Vol. 3, No. 6, 950–958, 2009.
12. Cameron, R. J., C. M. Kudsia, and R. R. Mansour, *Microwave Filters for Communication Systems*, Wiley, Hoboken, NJ, 2007.
13. Hong, J. S. and M. J. Lancaster, *Micrsotrip Filters for RF/Microwave Applications*, Wiley, New York, NY, 2001.
14. Sun, J. J., S. Sun, X. Yu, Y. P. Chen, and J. Hu, "A deep neural network based tuning technique of lossy microwave coupled resonator filters," *Microwave and Optical Technology Letters*, Vol. 61, No. 9, 2169–2173, 2019.
15. Şenel, B. and F. A. Şenel, "Bandpass filter design using deep neural network and differential evolution algorithm," *Arabian Journal for Science and Engineering*, Vol. 47, 14343–14354, 2022.
16. Roshani, S., H. Heshmati, and S. Roshani, "Design of a microwave lowpass — Bandpass filter using deep learning and artificial intelligence," *Journal of the Institute of Electronics and Computer*, Vol. 3, No. 1, 1–16, 2021.
17. Hong, J. S., "Couplings of asynchronously tuned coupled microwave resonators," *IEE Proceedings: Microwaves, Antennas and Propagation*, Vol. 147, No. 5, 354–358, 2000.

18. Liu, S., J. Li, S. H. Hwang, H. K. Son, and Y. J. Chong, "Interference analysis method for 5G system to radio altimeter," *Asia Pacific Wireless Communications Symposium (APWCS)*, 80–84, 2022.